

Application of the Griffith criterion to fracture of boron fibres

JORGE VEGA BOGGIO, OLOF VINGSBO

Institute of Technology, Uppsala University, Uppsala, Sweden

Tensile tests were performed on boron fibres and the resulting fracture stresses σ_f recorded. The fracture surfaces were investigated by SEM, with emphasis on the type of flaw nucleating the fracture. It was found that pre-existing, so-called proximate voids, in the boron mantle near the core-mantle interface, have transverse irregularities, large enough to create stress concentrations. The radial extensions, $2c$, of fracture initiating proximate voids in mirror zones were measured from the micrographs. The obtained $2c-\sigma_f$ relation was found to be in good agreement with the Griffith criterion for brittle fracture. In addition, the experimental $\log 2c-\log \sigma_f$ plot gives some information on the value of the surface energy, γ , of boron.

1. Introduction

1.1. Fracture types in boron fibres

Boron fibres fracture in tension in a brittle manner. The fracture surfaces are very similar to those of glass rods, and can even be divided into mirror, mist and hackle zones, with the aid of which the crack nucleation site can be traced [1-4]. Fracture is experimentally known to nucleate at imperfections ("flaws") of different types, some of which can be controlled by the manufacturing conditions.

With some generalization, fracture types are classified in relation to the type of initiating flaw, namely [4] (i) surface flaws, (ii) radial cracks, or (iii) "proximate voids" (pores near the core-mantle interface). In addition, transverse cracks can nucleate homogeneously within the apparently perfect core.

There is a strong correlation between the tensile strength and the type of fracture, expressed by Line and Henderson [1] as an inverse proportionality between the fracture stress, σ_f , and the "severity" of the triggering flaw. They also suggested the possibility of crack nucleation at pre-existing internal flaws, according to the Griffith criterion for fracture of glasses [2]. As far as we know, however, no attempt has been made to check this idea. The present work is an investigation of the possibility of applying the Griffith

model to the fracture of boron fibres, tested in tension.

1.2. The Griffith criterion

In his now classical work on brittle fracture, Griffith [2] suggested that an apparently homogeneous tensile test specimen might contain small defects, causing stress concentrations high enough for the ideal fracture stress to be attained in localized regions. If the defect is a flat, elliptical void in a plane normal to the direction of the applied stress, with the major axis $2c$, fracture will occur for the applied stress

$$\sigma_f = \left(\frac{2E\gamma}{\pi c} \right)^{1/2} \quad (1)$$

where E is Young's modulus and γ is the surface energy of the failing material.

The Griffith criterion is based on the two requirements that (i) the material is truly brittle, i.e. fractures in a glass-like manner, and (ii) the material contains pre-existing imperfections of the geometry of a Griffith crack.

2. Experimental

2.1. Material

Continuous fibres, laboratory-produced in multi-stage processes by two manufacturers (A and B) under highly varied conditions, were investigated.

The outer diameters were roughly the same, 106 μm (A) and 90 μm (B) respectively.

2.2. Tensile testing

30 tensile specimens from an A spool, 30 specimens from a B spool and 100 specimens from a second B spool were tested in a Lorentzen and Wettres (ALLWETRON) micro-tensile test machine. The specimens had a gauge length of 25 mm and were mounted between a sheet of paper and adhesive tape in order to retain the debris after fracture. The contact between the grips and the fibres was improved by the use of emery paper. The fibre diameters were determined with a Mikrokator.

2.3. Morphology

Fractured fibres were mounted in a specially made, rotatable and tiltable holder for SEM specimens. The specimens were washed successively in trichlorethylene, acetone and alcohol, given a thin gold coating by sputtering and studied in a JSM-U3 scanning electron microscope, operated at 20 kV. Ten additional specimens of 50 mm length were cut at random from each spool, and given an electrolytical coating of nickel. The resulting composite was polished, ion-etched and studied in longitudinal sections in a JEM 200 B scanning transmission electron microscope, operated at 200 kV.

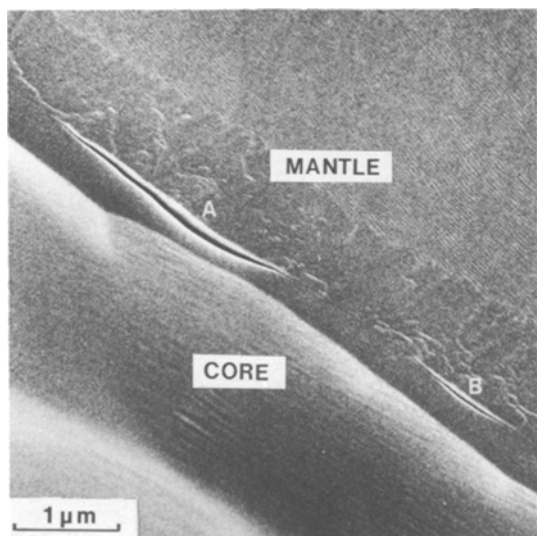


Figure 1 200 kV SEM micrograph of longitudinal section. (along the line indicated in Fig. 2) showing two axially elongated voids at A and B (B fibre).

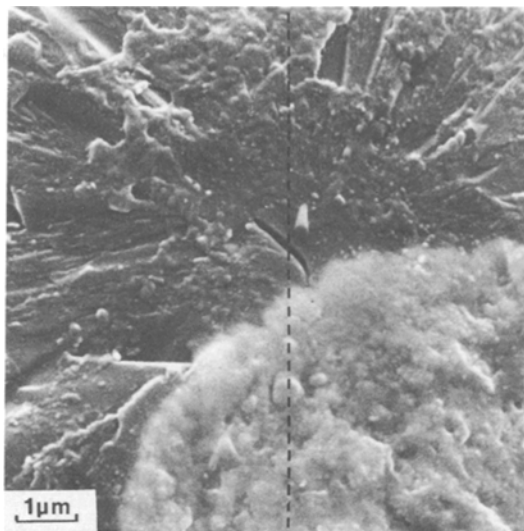


Figure 2 20 kV SEM micrograph of proximate void initiated fracture (B fibre, $\sigma_f = 36.4 \times 10^2 \text{ N mm}^{-2}$). The line gives approximately the plane of the longitudinal section of Fig. 1.

3. Proximate voids

3.1. Definition

Proximate voids are defined as pores in the boron mantle, in the immediate vicinity of the core–mantle interface. They may be the result of vacancy condensation according to a diffusion mechanism, discussed qualitatively by Wawner [5], and supported quantitatively in an experiment by Vega Boggio and Vingsbo [4].

These voids have been observed in fracture surfaces as well as in sections of non-tested fibres, which indicates that this type of imperfection can exist before a mechanical test.

3.2. Morphology

SEM studies of transverse and axial (Fig. 1) sec-

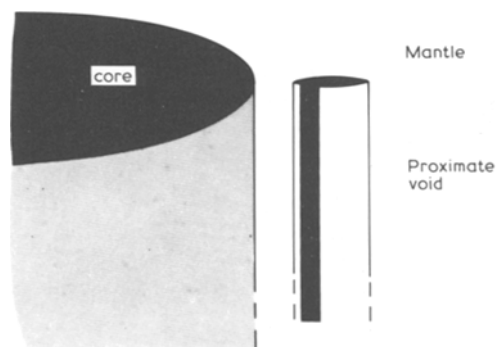


Figure 3 The general morphology of a proximate void.

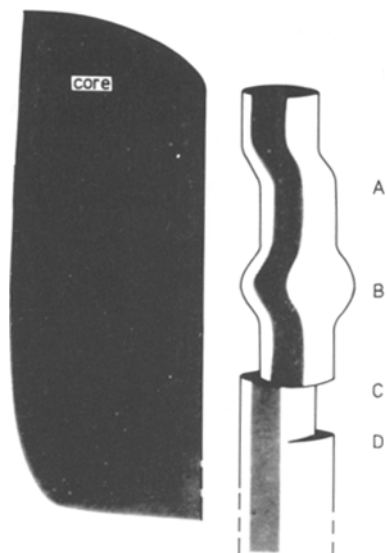


Figure 4 Schematic representation of shape irregularities in proximate voids: bend (A), bulge (B) and surface steps (C and D).

tions, and of essentially transverse fracture surfaces (Fig. 2), give the general three-dimensional shape of proximate voids schematically shown in Fig. 3, with a radial dimension of the order of $1\ \mu\text{m}$ and, often, a considerably longer axial extension.

Two types of shape irregularities may be large enough for creating stress concentrations, (see Figs. 4 and 5):

(i) local radial surface curvature, giving rise to bends or bulges (A and B in Fig. 4);

(ii) surface steps (C and D in Figs. 4, 5a and b)

3.3. Application of the Griffith model

The void morphology described above suggests the possibility of Griffith crack formation under a normal stress along the fibre axis at (i) bulges or (ii) surface steps. Therefore, fracture surface pairs were chosen, on which hackle marks and mirror zones indicated crack nucleation just outside the core-mantle interface. It generally proved possible to find a proximate void in at least one of the two fracture surfaces. Sometimes the latter coincided with a step, as in Fig. 5. If not, it was assumed that the fracture surfaces corresponded to a bulge. The critical parameter $2c$, the major axis of the Griffith crack, was measured as the extension of the bulge, or of the stepped void, in the plane of crack propagation.

Proximate voids were first identified in SEM under the best imaging conditions, i.e. with a tilted specimen. In order to perform accurate measurements, the specimen was then brought to a normal position, and $2c$ was measured either directly on the CRT or on recorded photographs. Images from untilted specimen surfaces, however, had a relatively poor contrast. Therefore, the micrographs presented here, mainly having a demonstrative purpose, were taken at relatively high tilt angles, while the apparent dimensions of the voids do not

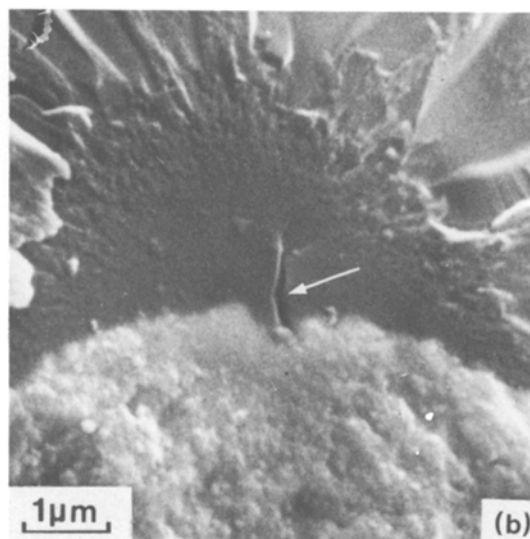
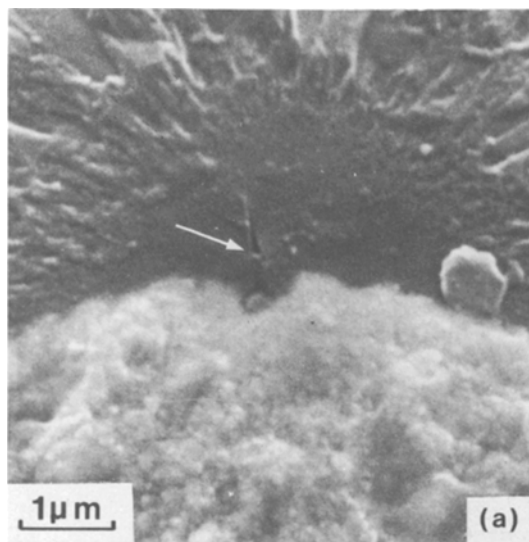


Figure 5 20 kV SEM micrographs of proximate void initiated fracture (B fibre, $\sigma_f = 31.5 \times 10^2\ \text{N mm}^{-2}$). Fracture was nucleated at a surface step of the D type in Fig. 4. It is clearly seen that part of the void in one of the fracture surfaces (b) terminates at the arrow and does not continue across the other fracture surface (a).

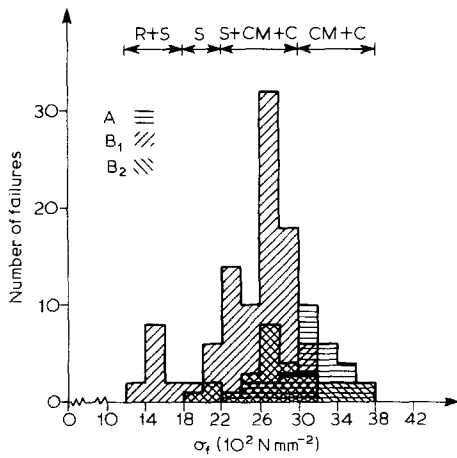


Figure 6 Histograms of the fracture stresses for spools A, B₁ and B₂. Above the histograms, the crack nucleation mechanisms have been grouped in relation to fracture stress intervals. The following abbreviations are used. R: radial crack, S: surface flaws, CM: proximate void and C: core.

necessarily correspond to the measured values.

A second important factor, taken into account for the measurements, was the variation of magnification with deviation from the pre-calibrated working distance. Because the pieces of fractured fibres, mounted in the specimen holders, varied in length, individual magnification corrections were made.

4. Results

A histogram of the obtained fracture stresses is reproduced in Fig. 6. The fracture mechanisms were grouped and related to fracture stress intervals as shown in the figure.

Table I shows the results of the $2c$ measurements. For comparison, proximate void type

TABLE I Proximate void transverse length $2c$ (μm) as a function of σ_f (10^2 N mm^{-2}). The values marked * are from Layden [3].

σ_f	$2c$	σ_f	$2c$	σ_f	$2c$	σ_f	$2c$
16.8	2.8*	27.0	1.6	29.1	1.5	31.9	1.2
24.6	2.0	27.2	1.8	29.6	1.4	31.9	1.1
24.6	1.8	27.4	1.7	29.6	1.2	32.7	1.2
25.3	2.2	27.8	1.8	29.7	1.3	33.0	1.1
25.3	2.1	27.8	1.6	29.7	1.4	33.0	1.1
25.5	1.6*	28.1	2.0	30.4	1.5	33.9	1.2
25.7	2.1	28.1	1.4	31.3	1.4	34.2	1.1
26.1	1.9	28.1	1.7	31.4	1.2	35.1	1.2
26.2	1.7	28.6	1.6	31.5	1.3	35.3	1.0
26.3	1.8	28.9	1.5	31.5	1.0	36.4	1.3
26.9	1.9	29.0	1.4	31.7	1.3	36.5	1.0

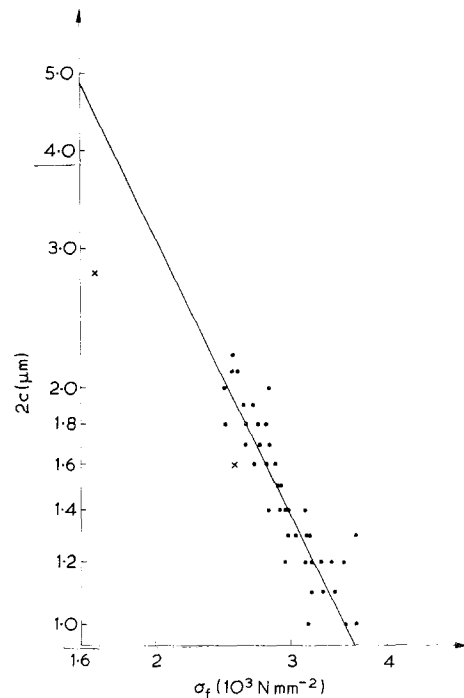


Figure 7 Logarithmic $2c$ - σ_f plot. The points represent the experimental values of Table I. The line corresponds to $\gamma = 22 \text{ J m}^{-2}$ (for $E = 4.4 \times 10^5 \text{ N mm}^{-2}$).

flaws, appearing in a paper by Layden [3], have been measured and included in Table I. The measurements were made directly on images in [3], and corrected for the tilt angle, which could be estimated from the ellipticity of the core image. $2c$ has been plotted versus σ_f in the log-log diagram of Fig. 7. It can be seen that the points fit reasonably well to the straight line.

5. Discussion

The characteristics of the Griffith law are that it yields a straight line in a log-log plot, the slope of which is -2 . Undoubtedly, the Griffith criterion is in good agreement with the present experimental results, which indicates that proximate void irregularities can act as Griffith cracks. The relatively good agreement with the points derived from Layden's work [3], further supports this idea. In addition, an extrapolation to $2c = 100 \mu\text{m}$ (the whole fibre diameter) gives the corresponding minimum fracture stress $\sigma_f = 300 \text{ N mm}^{-2}$, which is definitely lower than any observed fracture stress.

The position of the Griffith line directly depends on the E and γ values. With experimental

Young's moduli it is then possible to calculate the surface energy.

The generally accepted E value for boron fibres, $4 \times 10^5 \text{ N mm}^{-2}$, corresponds to measurements on whole fibres, including the tungsten boride core. In the present case, however, the crack being nucleated in the mantle, this value is not necessarily relevant.

An approach to improve E measurements is to increase the fibre-to-core diameter ratio, which in commercial fibres is fixed to approximately 5:1. By growing a fibre of $1000 \mu\text{m}$ o.d. on a tungsten wire of $25 \mu\text{m}$ diameter, Talley [6] minimized the effect of the core. No value was given of the final diameter (after diffusional growth) of the core, but Talley's result $E \approx 4.4 \times 10^5 \text{ N mm}^{-2}$ seems to be the most accurate value available.

The corresponding surface energy then is $\gamma = 22 \text{ J m}^{-2}$, which is around 3 to 7 times higher than available literature values for bulk tungsten [7, 8]. Considering the known differences in γ values obtained by bulk and fibre measurements, this seems quite reasonable.

Acknowledgements

The authors wish to express their gratitude to Fil.Lic. Tommy Lindahl, Fil.Mag. Jan Otto

Carlsson, Docent Axel Rönquist and Docent Torsten Lundström for stimulating advice and help. Thanks are also due to Ingrid Strandh for beautiful drawings and to Jim Musiol and Rein Kalm for skillful technical assistance. The tensile testing was performed at LUMALAMPAN AB, Stockholm.

References

1. L. E. LINE JUN. and U. V. HENDERSON JUN., in "Handbook of fiberglass and Advanced Plastic Composites", edited by G. Lubin (Van Nostrand Reinhold, New York, 1969).
2. A. A. GRIFFITH, *Phil. Trans. Roy. Soc.* **221A** (1920) 163.
3. G. K. LAYDEN, *J. Mater. Sci.* **8** (1973) 1581.
4. J. VEGA BOGGIO and O. VINGSBO, *ibid* **11** (1976) 273.
5. F. E. WAWNER JUN., in "Modern Composite Materials", edited by L. J. Broutman and R. H. Krock (Addison Wesley, Massachusetts 1967).
6. C. P. TALLEY, *J. Appl. Phys.* **30** (1959) 1114.
7. A. KELLY, "Strong Solids" (Clarendon Press, Oxford, 1966).
8. J. Å. SCHWEITZ and O. VINGSBO, *Mater. Sci. Eng.* **8** (1971) 275.

Received 9 March and accepted 3 May 1976.